Jurnal Akta Kimia Indonesia
INDONESIA CHIMICA ACTA

PAPER

View Article Online
View Journal View Issue

Cite this: *Indo. Chim. Acta.*, 2024, **17**, **2**.

Received Date: 9th July, 2024
Accepted Date: 30th December, 2024

Keywords:
EGFR;
Molecular Docking;
ADMET;
Drug-likeness;
Fisetin.

DOI: http://dx.doi.org/10.70561/ica.v17i2.35928

In Silico Insight of Natural Compounds in *Ageratum Conyzoides* L as Anti Breast Cancer Candidate by Molecular Docking Against EGFR

Putra Jiwamurwa Pama Tjitda[1]*, Tutik Dwi Wahyuningsih[2], and Febri Odel Nitbani[3]

Abstract. The regulation of proliferation and apoptosis in cancer cells, particularly breast cancer, hinges on the control exerted by the epidermal growth factor receptor (EGFR). Naturally derived EGFR inhibitors from natural compounds show significant potential for future advancements. This study aims to assess the efficacy of active compounds found in *Ageratum conyzoides* L. as EGFR inhibitors. Evaluation involved molecular docking studies of active compounds, namely flavonoid, chromene, terpene, sterol, and acid compound derivatives, against EGFR using PDB ID 1m17. Additionally, the ADMET properties and drug-like characteristics of the most promising compounds were characterized. Findings reveal that compound C2 (Fisetin) exhibits the most favorable binding energy of -8.9 kcal/mol. Fisetin establishes crucial interactions, particularly with the catalytic site at Met769 of the hinge protein. Fisetin also engages in hydrophobic interactions in regions I and II, involving Val702, Leu694, and Leu820. ADMET profiling of fisetin demonstrates favorable attributes, suggesting its potential as a promising anticancer agent based on drug-likeness assessments.

Introduction

Breast cancer is among the leading causes of death in women worldwide. According to the World Health Organization (WHO, 2024), breast cancer was reported in women across 157 out of 185 countries globally in 2022. This disease has resulted in approximately 670 million deaths globally during the same year. Despite women being at higher risk for this disease, approximately 0.5% to 1% of cases globally are diagnosed in men. Meanwhile, the Ministry of Health of Indonesia notes that breast cancer contributes significantly, comprising 16.6% or 68 million of total detected cancer cases (Kementerian Kesehatan RI, 2022).

Tyrosine kinase receptors such as the epidermal growth factor receptor (EGFR) are known to play a crucial role in various cellular developments. Overexpression of EGFR activity can trigger cancers, such as breast cancer, as this receptor influences cell signaling pathways and proliferation (Yang et al., 2023). Under these conditions, EGFR phosphorylates PELI1, leading PELI1 to undergo polyubiquitination. Consequently, cell metastasis promotes the onset of breast cancer (Qi et al., 2023). Dysfunction of EGFR inhibits gene amplification and overexpression of EGFR, thus preventing cancer metastasis.

Several drugs clinically proven as anticancer agents, such as erlotinib, are utilized in chemotherapy. These drugs operate by inhibiting EGFR autophosphorylation through competitive inhibition of ATP binding (Singh & Bast, 2014). However, recent research findings indicate a decline in the effectiveness of erlotinib in breast cancer treatment. Erlotinib induces phosphorylation of p27 at Ser10, leading to resistance against EGFR inhibition. Moreover, erlotinib has been found to interact with ABC transporters responsible for drug efflux, necessitating combination therapy approaches in cancer treatment. Therefore, the development of new compounds as potential anticancer candidates is imperative.

The exploration of natural compounds in the discovery of new drugs is currently intriguing for investigation. The chemical diversity and biological activities of natural

[1]*Department of Pharmacy, Health Polytechnic of Kupang, Kupang, 85111, Indonesia;* ***Email: putrachemist_jc@yahoo.com***
[2]*Department of Chemistry, Faculty of Mathematics and Natural Sciences, Universitas Gadjah Mada, Yogyakarta, 55281, Indonesia.*
[3]*Department of Chemistry, Faculty of Science and Engineering, University of Nusa Cendana, Kupang, 85001, Indonesia.*

compounds offer significant potential in drug development (Mudunuru et al., 2023). Bandotan plant (*Ageratum conyzoides* L.) contains various groups of natural compounds. Therefore, it has shown biological activities including anti-inflammatory effects (Vikasari et al., 2022), antibacterial properties (Aernan et al., 2024), and antifungal activity (Nguyen et al., 2021).

Previous studies have shown that the chloroform fraction of *Ageratum conyzoides* L. can inhibit the HeLa cell line, with an IC_{50} value of 30 µg/mL based on a single cytotoxic assay, and the binding affinity of nobiletin, identified as an active compound, was reported to be -8.0 kcal/mol (Febriansah & Komalasari, 2019). Furthermore, the extract of *Ageratum conyzoides* L. exhibited promising anti-breast cancer activity, with IC_{50} values of 64 µg/mL, 22 µg/mL, and 163 µg/mL against matrix metalloproteinase-9 (MMP-9), 4T1, and T47D cell lines, respectively. The binding energy of sesamin, identified as another active compound, was predicted to be -8.3 kcal/mol based on in silico analysis. However, confirmation through GC-MS profiling revealed the absence of sesamin, suggesting that other compounds may contribute to its observed activity (Hariono et al., 2020).

On the other hand, several active compounds have been identified in the extract of *Ageratum conyzoides* L., including flavonoids, chromenes, terpenes, sterols, and acidic compounds (Yadav et al., 2019). The diversity of these active compounds offers valuable insights into the potential of this plant as a candidate for anti-breast cancer therapy. Molecular docking, a computational method, plays a pivotal role in accelerating drug discovery and optimizing lead compounds. This technique predicts binding energies and chemical interactions between small molecules and receptor binding sites (Cheng et al., 2023).

In this study, the group of active compounds found in *Ageratum conyzoides* L. (Figure 1), including flavonoids, chromenes, terpenes, sterols, and acids, were investigated for their inhibitory activity against EGFR through molecular docking. The binding energy and chemical interactions of all active compounds were evaluated and studied. Furthermore, the pharmacokinetic properties and drug-likeness of the best compounds identified from this screening were assessed.

Experimental

Material and Methods

The computational study utilized hardware powered by a Core i9-13900H processor. Software tools employed for preparing the structures of test compounds included ChemDraw Professional and Chem3D. Molecular docking studies were conducted using AutoDock Vina facilitated by the AutoDock tools interface. Chemical interaction visualizations from molecular docking were generated using Discovery Studio Client 2021.

Procedures

Ligand Preparation

Active compounds found in the plant *Ageratum conyzoides* L. were obtained through literature studies (Yadav et al., 2019). The preparation of tested compounds began with sketch the structure of each tested compound and converting them into 3D structures using Chemdraw Professional and Chem3D. All these compounds were structurally optimized using the MM2 method. The optimized structures were converted from PDB format to pdbqt using Open Babel software.

Protein Receptor Preparation

The preparation of the receptor protein, Epidermal Growth Factor Receptor (EGFR) with PDB code 1m17, was obtained from the RCSB website. Subsequently, water molecules were removed from the protein structure. The native ligand, erlotinib, was extracted. The protein structure was then prepared by adding polar hydrogen atoms and Kollman charges. This preparation process utilized AutoDock tools. The prepared protein structure was saved in pdbqt format.

Molecular Docking

The molecular docking protocol of the tested compounds was conducted following the protocol from previous studies (Chunaifah et al., 2024). Each prepared test compound was docked onto EGFR using an exhaustiveness parameter set to 100. The grid center settings for X, Y, and Z coordinates were 21.697, -0.022, and 52.186, respectively, with a grid box size of 16 Å. The inhibitory activity against EGFR of the tested compounds was determined based on binding energy and observation of chemical interactions with essential amino acid residues within the binding pocket.

Profile ADMET and Drug-Likeness Evaluation

The best compound based on the results of molecular docking was further evaluated for its pharmacokinetic characteristics in silico. ADME properties were determined by inputting the SMILES notation of the best compound into the pkCSM web tool (https://biosig.lab.uq.edu.au/pkcsm/prediction).

Subsequently, its toxicity profile was assessed using ProTox-3 (https://tox.charite.de/protox3/). Drug-likeness characteristics of the best compound were determined

using SwissAdme (http://www.swissadme.ch/), and the drug-likeness score was established using the Molsoft tool (https://molsoft.com/mprop/).

Result and Discussion

Molecular Docking

The evaluation of the potential of active compounds found in *Ageratum conyzoides* L. as anticancer agents was studied in silico. EGFR is a tyrosine kinase receptor that plays a crucial role in cancer growth, particularly in breast cancer. EGFR is involved in gene transcription, leading to increased cell proliferation. Cellular damage caused by chemotherapy is protected by EGFR activity, thereby inducing resistance to most anticancer drugs (de Araújo et al., 2022). Inactivation of EGFR can inhibit proliferation and division of cancer cells. Therefore, this receptoris crucial for exploring anticancer drug candidates.

In this study, several groups of active compounds such as flavonoids, chromenes, monoterpenes, sterols, and acid derivatives were investigated for their inhibitory activity against EGFR (Table 1). The co-crystal structure of EGFR and FDA-approved drug erlotinib was used as a reference compound to evaluate the inbibitory activity of active compounds. Molecular docking of erlotinib yielded a binding energy of -7.9 kcal/mol. Chemical binding at the hinge position of EGFR is indicated by the interaction of the quinazoline ring N1 with Met769 (Figure 2) (Yang et al., 2023). The hydrophobic interactions in regions I and II as the catalytic sites of EGFR are displayed by erlotinib (Singh & Bast, 2014). The amino acids Val702 and Leu764 in hydrophobic region I are facilitated by pi-alkyl interactions, while Leu694 and Leu820 in hydrophobic region II are bound through pi-alkyl and pi-sigma interactions.

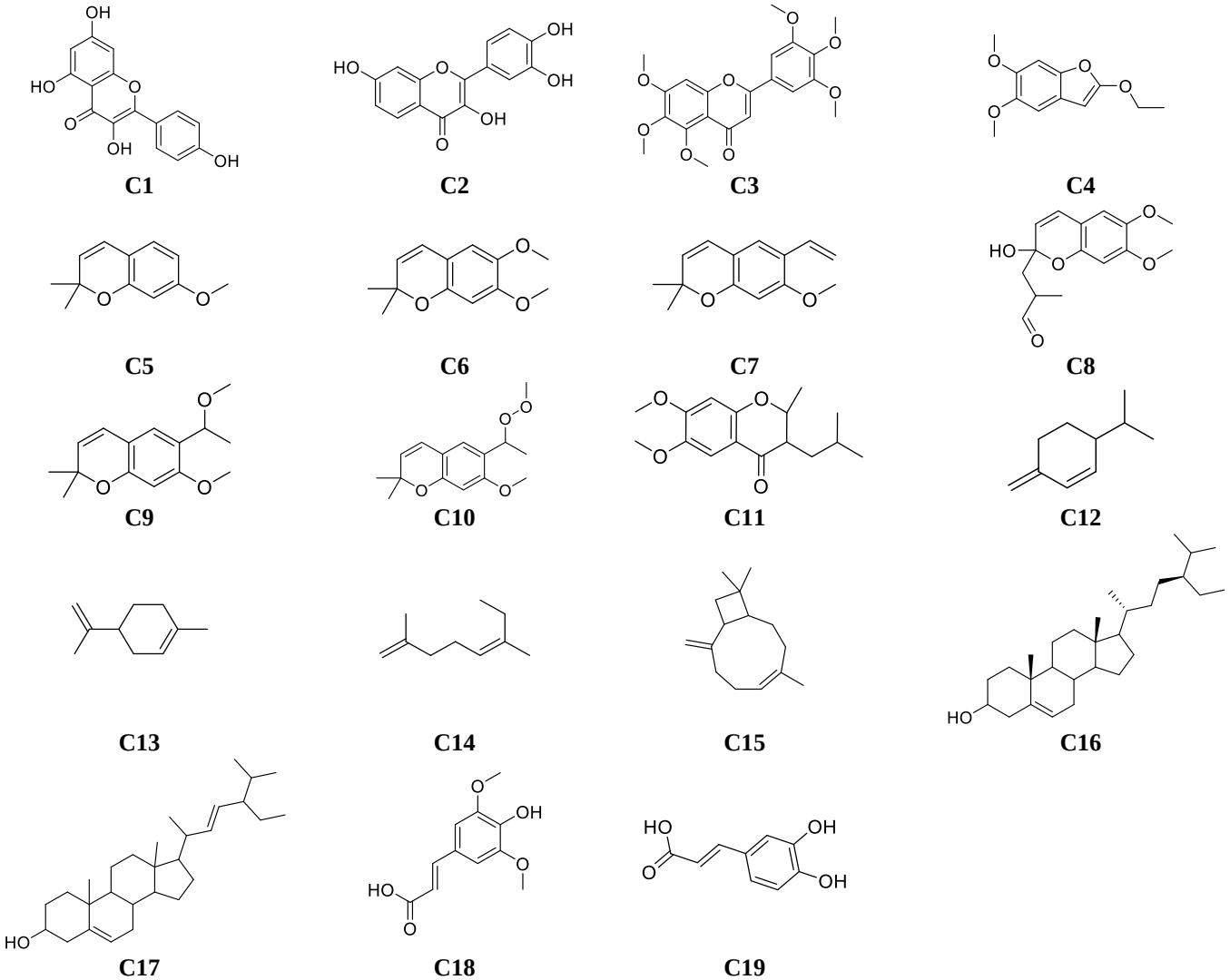

Figure 1. Chemical structure of active compounds in *Ageratum conyzoides* L.

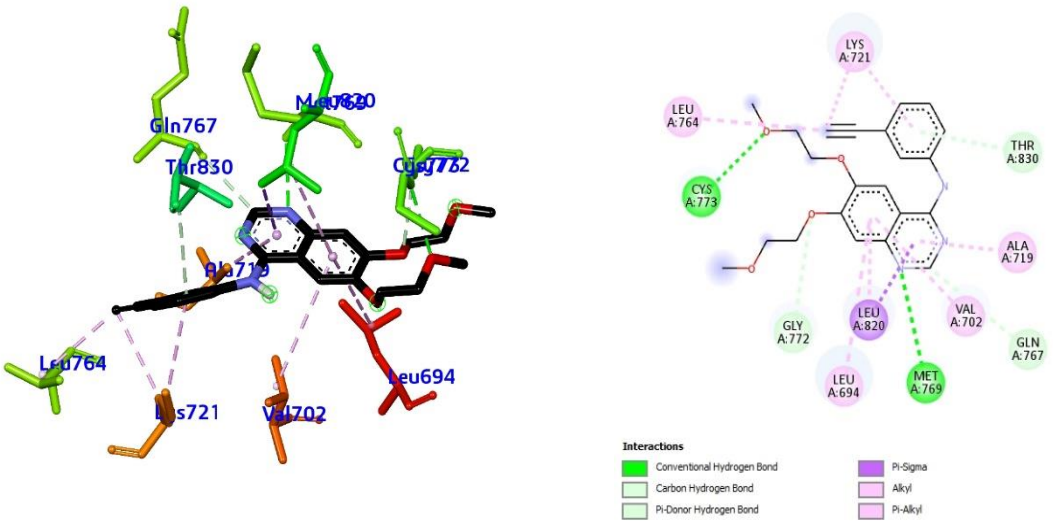

(a) **(b)**

Figure 2. Depiction of the chemical interactions of erlotinib compound in the EGFR binding pocket **(a)** 3D and **(b)** 2D visualization.

Table 1. Chemical interaction of active compound in *Ageratum conyzoides* L.

ID Compound	IUPAC Name	Interaction	
		Hydrogen bond (distance, Å)	Hydrophobic
Erlotinib	N-(3-ethynylphenyl)-6,7-bis(2-methoxyethoxy)quinazolin-4-amine	Gln767 (3.36), Met769 (3.12), Gly772 (3.47), Cys773 (3.05), Thr830 (4.01)	Leu694, Val702, Ala719, Lys721, Leu764, Leu820
	Flavonoid		
C1	3,5,7-trihydroxy-2-(4-hydroxyphenyl)chromen-4-one	Ala719 (2.12), Thr766 (3.49), Thr830 (3.03)	Val702, Lys721, Leu820
C2	2-(3,4-dihydroxyphenyl)-3,7-dihydroxychromen-4-one	Glu738 (2.03), Thr766 (3.00), Gln767 (2.51), Met769 (2.84), Thr830 (2.87)	Leu694, Val702, Ala719, Lys721, Leu820
C3	5,6,7-trimethoxy-2-(3,4,5-trimethoxyphenyl)chromen-4-one	Lys721 (3.02), Glu738 (3.39), Thr766 (3.14), Thr830 (3.50)	Leu694, Phe699, Val702, Ala719, Leu768, Leu820, Asp831
C4	2-ethoxy-5,6-dimethoxybenzofuran	Cys751 (3.73), Thr766 (2.98), Met769 (3.45)	Leu694, Val702, Ala719, Lys721, Met742, Leu764, Leu768, Leu820
	Chromene		
C5	7-methoxy-2,2-dimethylchromene	Thr766 (2.81), Met769 (3.37)	Leu694, Val702, Ala719, Lys721, Leu768, Leu820
C6	6,7-dimethoxy-2,2-dimethylchromene	Thr766 (2.96), Met769 (3.43)	Leu694, Val702, Ala719, Leu768, Leu820
C7	6-ethenyl-7-methoxy-2,2-dimethylchromene	Thr766 (2.94), Met769 (3.73)	Leu694, Val702, Ala719, Lys721, Leu768, Leu820
C8	3-(2-hydroxy-6,7-dimethoxy-2H-chromen-2-yl)-2-methylpropanal	Thr830 (2.72), Asp831(3.98)	Phe699, Val702

ID Compound	IUPAC Name	Interaction	
		Hydrogen bond (distance, Å)	Hydrophobic
C9	7-methoxy-6-(1-methoxyethyl)-2,2-dimethylchromene	Thr766 (2.93)	Val702, Ala719, Leu820
C10	7-methoxy-2,2-dimethyl-6-(1-(methylperoxy)ethyl)-2H-chromene	-	Val702, Ala719, Lys721, Leu820
C11	3-isobutyl-6,7-dimethoxy-2-methylchroman-4-one	Thr766 (2.86), Gln767 (3.45), Asp831 (3.53)	Phe699, Val702, Ala719, Lys721, Met742, Leu764, Met769, Leu820
	Terpenes		
C12	3-methylidene-6-propan-2-ylcyclohexene	-	Val702, Ala719, Lys721, Met742, Leu764, Leu820
C13	1-methyl-4-prop-1-en-2-ylcyclohexene	-	Val702, Ala719, Lys721, Met742, Leu764, Leu820
C14	(5Z)-2,6-dimethylocta-1,5-diene	-	Val702, Ala719, Lys721, Met742, Leu764, Leu820
C15	(4Z)-4,11,11-trimethyl-8-methylidenebicyclo[7.2.0]undec-4-ene	-	Val702, Leu820
	Sterols		
C16	(10R,13R)-17-((2R,5S)-5-ethyl-6-methylheptan-2-yl)-10,13-dimethyl-2,3,4,7,8,9,10,11,12,13,14,15,16,17-tetradecahydro-1H-cyclopenta[a]phenanthren-3-ol	Asp831 (4.56)	Val702, Arg817, Leu820
C17	17-[(E)-5-ethyl-6-methylhept-3-en-2-yl]-10,13-dimethyl-2,3,4,7,8,9,11,12,14,15,16,17-dodecahydro-1H-cyclopenta[a]phenanthren-3-ol	-	Phe699, Val702, Leu820
	Acids		
C18	(E)-3-(4-hydroxy-3,5-dimethoxyphenyl)prop-2-enoic acid	Glu738 (3.51), Lys721 (3.16), Met769 (3.04), Thr830 (3.58)	Val702, Met742
C19	(E)-3-(3,4-dihydroxyphenyl)prop-2-enoic acid	Lys721 (3.27), Met769 (3.21), Thr830 (2.91)	Val702, Ala719, Leu820

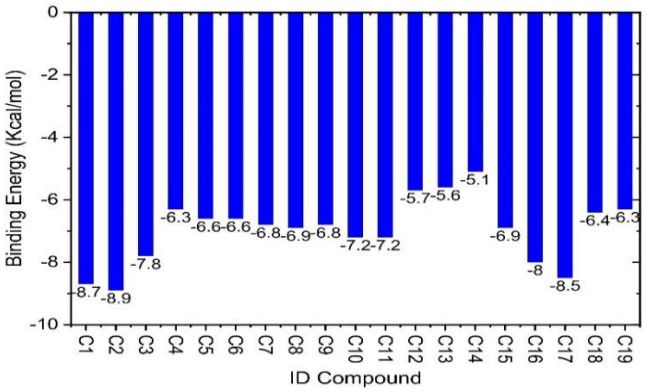

Figure 3. Binding energy of active compound in *Ageratum conyzoides* L.

Molecular docking of four flavonoid compounds against EGFR yielded respective binding energies for compounds C1, C2, C3, and C4 of -8.7, -8.9, -7.8, and -6.3 kcal/mol (Figure 3). Compound C2 exhibited the highest binding energy among the three other flavonoids. Chemical interaction analysis indicated hydrogen bonding between Met769 and the carbonyl oxygen atom (Figure 4). The bond distance of this interaction was lower (2.84 Å) compared to erlotinib (3.12 Å). Binding to the amino acid Val702 in hydrophobic region I occurred via pi-alkyl interactions. Complex stability was also aided by interactions in hydrophobic region II with amino acids Leu694 and Leu820 through pi-sigma interactions. Furthermore, the absence of Met769 interaction in compound C1 likely decreased the binding energy of the C1-EGFR complex. Although compound C4 was able to interact with Met765, it exhibited the lowest binding energy among the flavonoid group, possibly due to a larger bond distance (3.45 Å). Meanwhile, the C3-EGFR complex was stabilized solely through hydrophobic interactions.

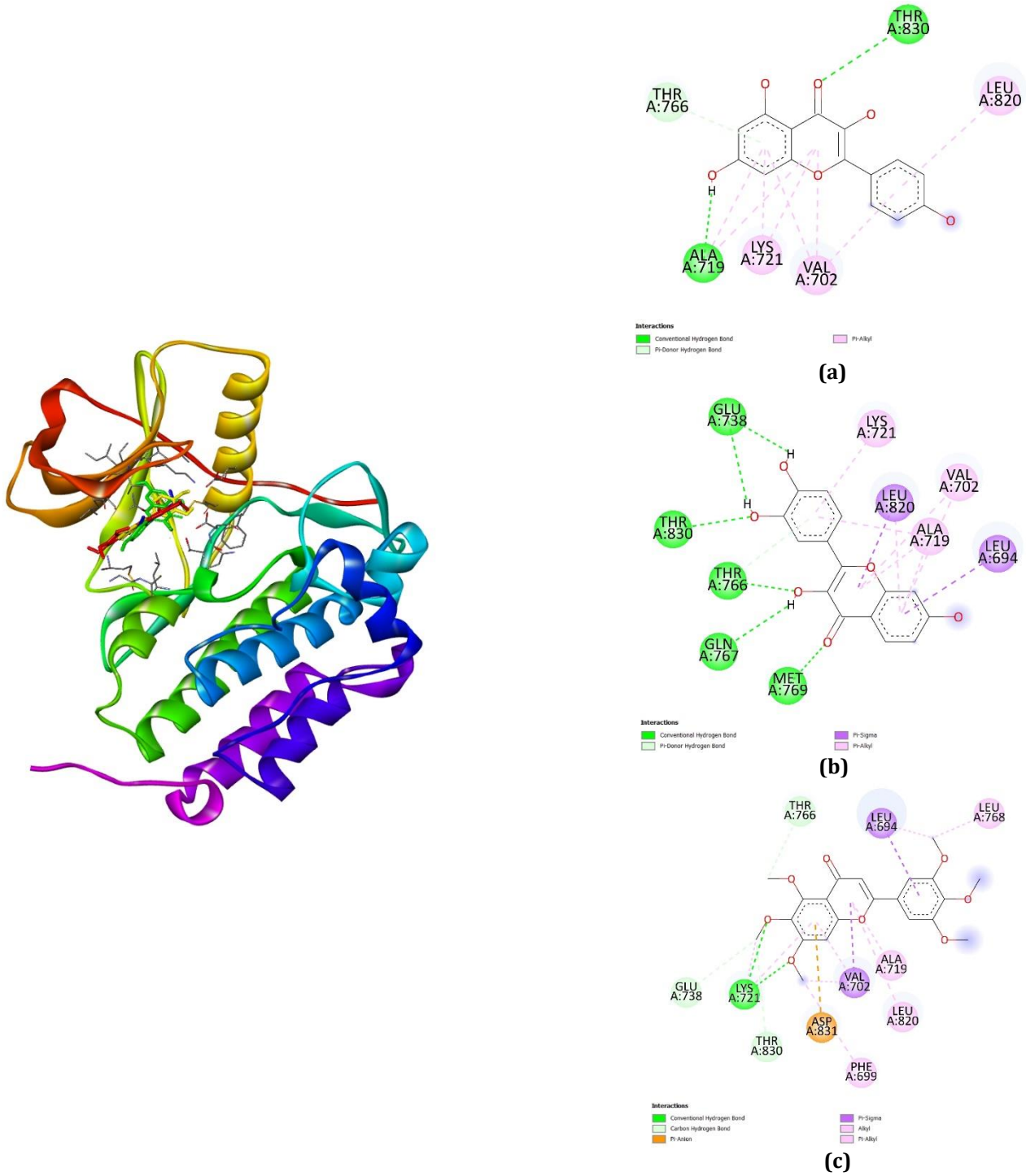

Figure 4. 3D and 2D chemical interaction of flavonoid groups **(a)** compound C1, **(b)** compound C2, and **(c)** compound C3.

For the chromene compound group (compounds C5-C11), compounds C10 and C11 exhibited the highest binding energy within their group at -7.2 kcal/mol. The stability of these complexes was predominantly governed by hydrophobic interactions with amino acids Val702, Met742, Leu764, and Leu820 (Figure 5). Interaction with Met769 was observed through alkyl interactions in compound C11, which were weaker than hydrogen bonds. Compound C8 showed a binding energy of -6.9 kcal/mol and formed only hydrophobic interactions with Val702. Meanwhile, compounds C5, C6, and C7 were observed to bind to Met769 through hydrogen bonding, with bond distances greater than 3.3 Å.

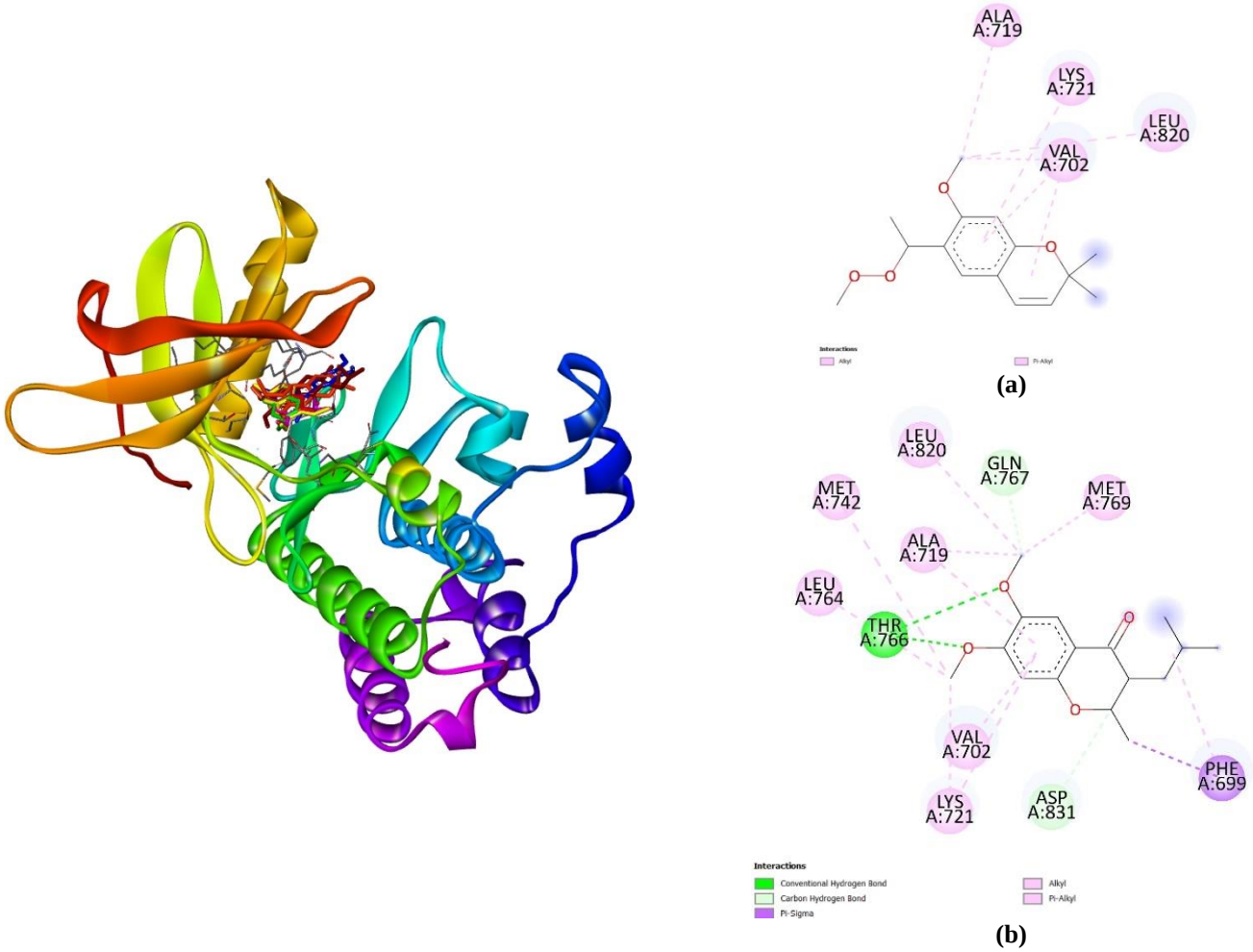

Figure 5. 3D and 2D chemical interaction of chromene groups **(a)** compound C10 and **(b)** compound C11.

The terpenes compound group (C12-C15) exhibited lower binding energies compared to other compound groups, ranging from -5.1 to -6.9 kcal/mol. Visualization of their interactions is presented in Figure 6. This group of compounds did not show interactions with Met769, which is the ATP binding site. The absence of these interactions is suspected to contribute to the lower binding energies observed. Interactions of these compounds with the EGFR binding site were stabilized solely through hydrophobic interactions I and II, involving amino acids Val702, Met742, Leu764, and Leu820, via alkyl interactions. Structurally, these compound groups lack functional groups is not capable of providing hydrogen bond interactions.

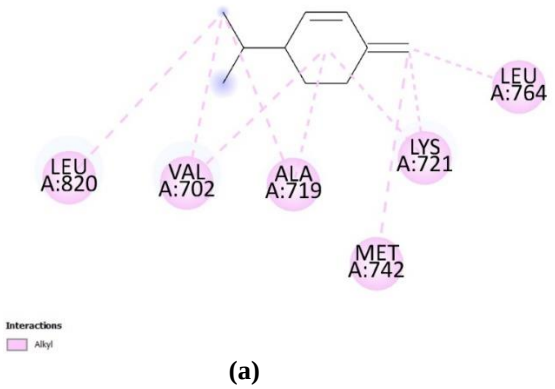

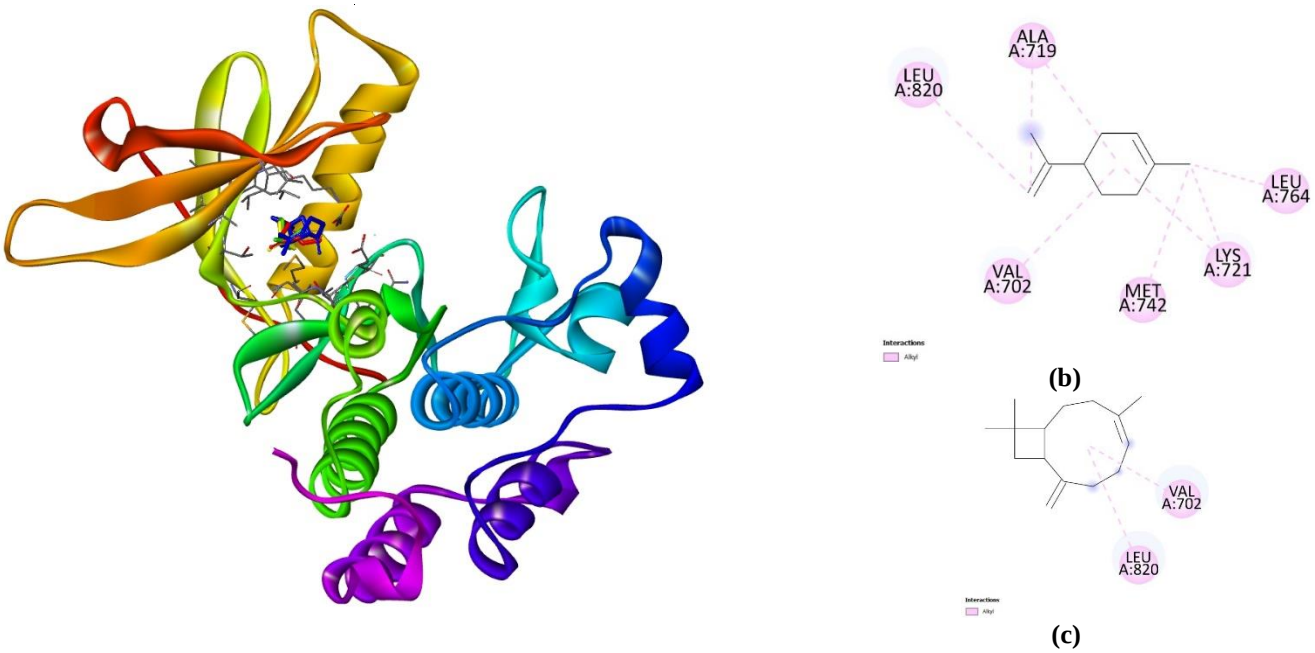

Figure 6. 3D and 2D chemical interaction of terpenes groups **(a)** compound C12, **(b)** compound C13, and **(c)** compound C15.

The sterol compound group provided satisfactory binding energies of -8.0 and -8.5 kcal/mol for compounds C16 and C17, respectively. The hydroxyl group in compound C16 bound to the amino acid Asp831 via a hydrogen bond. Additionally, compound C16 also formed hydrophobic interactions with Val702 and Leu820 through alkyl interactions (Figure 7). Meanwhile, compound C17 stabilized its interactions with EGFR solely through hydrophobic interactions with amino acid residues Val702 and Leu820.

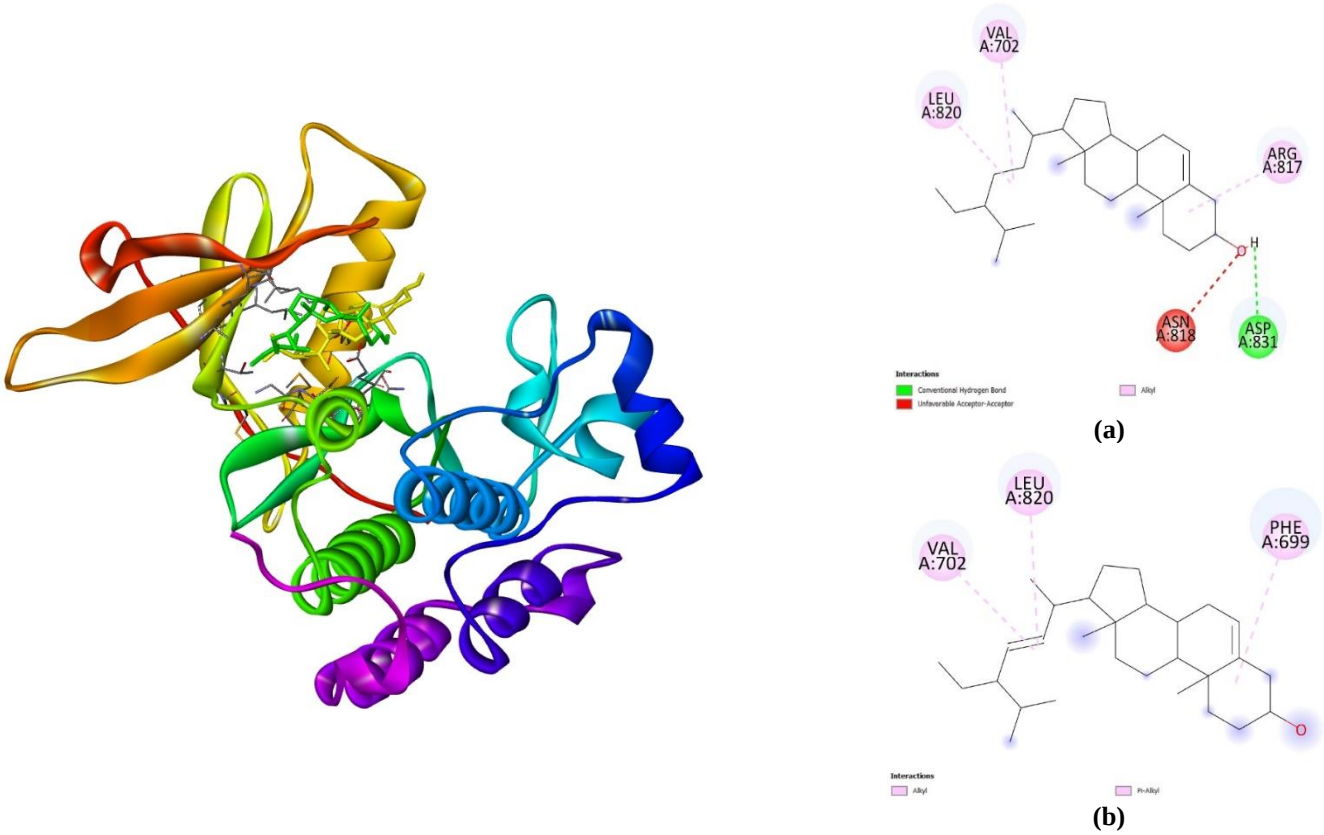

Figure 7. 3D and 2D chemical interaction of sterol groups **(a)** compound C16 and **(b)** compound C17.

For the acid compound group, the binding energies were -6.4 and -6.3 kcal/mol for compounds C18 and C19, respectively. The interactions of these compounds within the EGFR binding site are depicted in Figure 8. Compound C18 formed interactions with Met769 through hydrogen bonding, while complex stabilization was observed with Val702 and Met742 in hydrophobic region I via alkyl interactions. Compound C19 also showed hydrogen bonding interactions with Met769. However, the bond distance with Met769 in compound C19 was slightly larger than in compound C18, resulting in a slightly lower binding energy for compound C19 compared to compound C18.

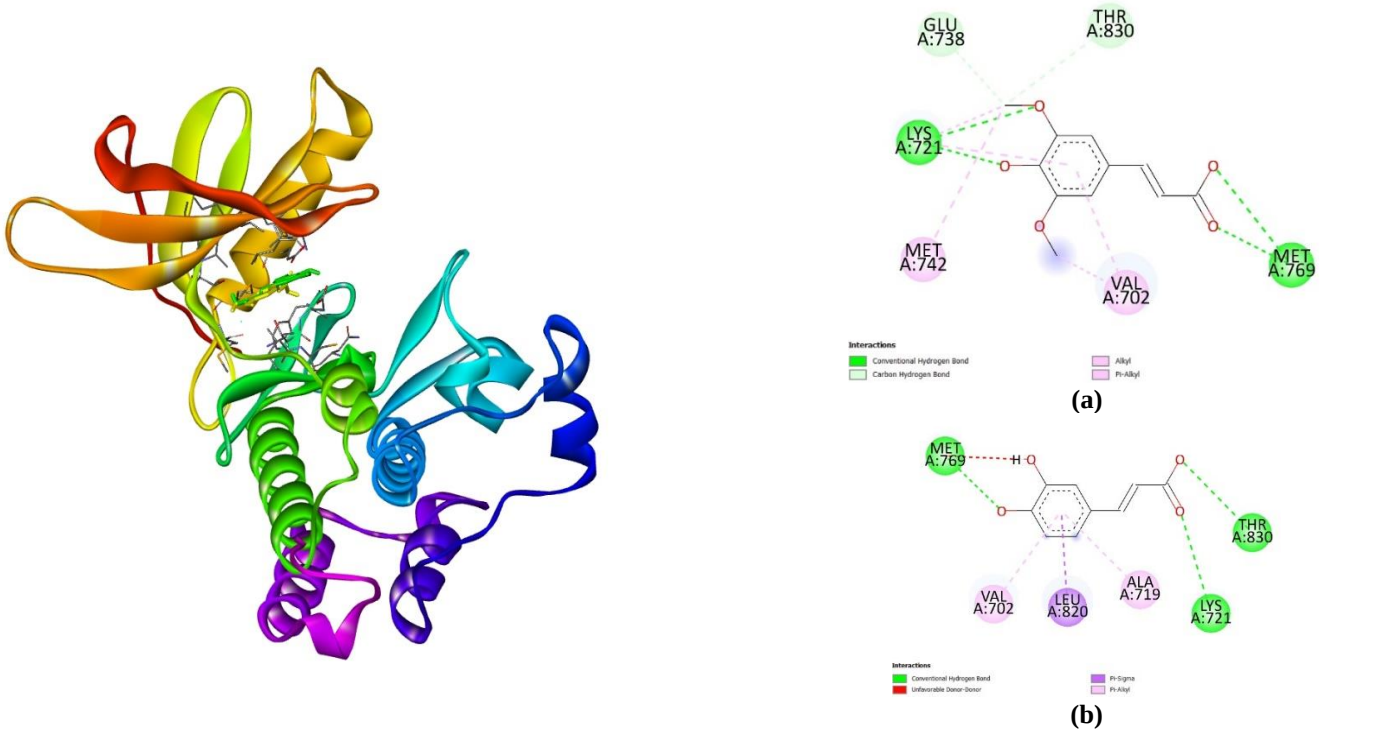

Figure 8. 3D and 2D chemical interaction of acid compound derivatives **(a)** compound C18 and **(b)** compound C19.

Profile ADMET and Drug-Likeness Evaluation

The adsorption, distribution, metabolism, and excretion characteristics of fisetin have been evaluated, and the results are presented in Table 2. Absorption is a crucial pharmacokinetic characteristic for predicting the bioavailability of a drug. The absorption properties of a compound significantly influence its therapeutic outcomes (Sim, 2015). The Caco2 permeability model is a value used to describe the potential gastrointestinal permeability of a compound (Falcón-Cano et al., 2022). This value is also used to illustrate the rate of absorption of a drug. The Caco2 permeability value of compound C2 is 0.377, falling into the medium category (high > 8 x 10-6 cm/s). Intestinal absorption predicts whether a drug can be taken orally. The predicted value for intestinal absorption of compound C2 is above 80%, indicating high intestinal absorption. Furthermore, the P-glycoprotein substrate parameter is crucial for describing a drug's ability to interact with ATP-binding cassette and relates to its potential for drug resistance (Lagares et al., 2019). Compound C2 acts as a substrate for P-glycoprotein, meaning that it can be transported by P-glycoprotein from cells, thereby enhancing its oral bioavailability.

Table 2. ADMET character of compound C2 (fisetin)

Parameter	Predicted value	Unit
Absorption		
Caco2 permeability	0.377	log Papp
Intestinal absorption	84.612	%
P-glycoprotein substrate	Yes	Categorical (Yes/No)
Distribution		
VDss	0.248	log L/kg
Fraction unbound	0.088	Fu
BBB permeability	-1.21	log BB

Parameter	Predicted value	Unit
CNS permeability	-2.407	log PS
Metabolism		
CYP2D6 substrate	No	Yes/No
CYP3A4 substrate	No	Yes/No
CYP2D6 inhibitor	No	Yes/No
CYP3A4 inhibitor	Yes	Yes/No
Excretion		
Total Clearance	0.492	log ml/min/kg
Renal OCT2 substrate	No	Yes/No
Toxicity		
AMES toxicity	No	Yes/No
Predicted LD_{50}*	159	mg/Kg
Predicted Toxicity Class*	3	Numeric

*measured by ProTox 3.0

Some of the distribution parameters evaluated include VDss, fraction unbound, BBB, and CNS permeability. Compound C2 has a VDss value of 0.248 log L/kg. This value falls within the medium range (-0.15<Vdss<0.45). VDss describes the proportion of a compound distributed in body tissues relative to blood plasma (Greenblatt, 2014). A high VDss value indicates a tendency for a drug to strongly bind to tissues, thus displaying therapeutic effects with minimal side effects. Next, fraction unbound (Fu) indicates the equilibrium between unbound and bound compound in plasma (Pires et al., 2015). The Fu value of compound C2 is 0.088. A high Fu value suggests that the compound is in an active form at high concentrations. Consequently, the compound exhibits high pharmacological activity but also high toxicity. Compound C2 has a low Blood-Brain Barrier (BBB) permeability category. This indicates that compound C2 has difficulty penetrating the BBB. Similar results are observed for Central Nervous System (CNS) permeability, where compound C2 shows a low value. This indicates that compound C2 faces challenges in crossing the CNS.

The metabolic capability of compound C2 was studied through its role as a substrate and inhibitor of isoforms of the cytochrome P450 enzyme such as CYP3A4 and CYP2D6. This information is crucial for future drug development purposes. The analysis results indicate that compound C2 only acts as an inhibitor of CYP3A4. This suggests that compound C2 has the potential to disrupt drug metabolism and drug-drug interactions (Samuels & Sevrioukova, 2021). Determining the total clearance of a drug is important to describe its removal capacity from the body. This value is often associated with the drug's bioavailability potential. Compound C2 has a total clearance value of 0.492 log ml/min/kg. A high total clearance value indicates that the compound is easily excreted from the body after metabolism. Meanwhile, the renal status of compound C2 as an OCT2 substrate is absent. This means that compound C2 tends not to interact with Organic Cation Transporter 2 (OCT2) and has the potential to interact with other drugs.

Determination of toxicity properties based on AMES toxicity assay showed that compound C2 is non-toxic. Confirmation of these results was further conducted using ProTox 3.0 webtools. The prediction results provided a predicted LD_{50} of 159 mg/kg. The toxicity characterization of compound C2 falls into class 3. Toxicity levels are categorized into several classes (Banerjee et al., 2024). Class 3 toxicity level indicates that the compound is predicted to be moderately toxic. Pharmacokinetic characteristics are also influenced by the drug-likeness profile of the studied compound. Evaluation of the drug-likeness profile of compound C2 has been conducted and the results are presented in Table 3. The predicted log P value of compound C2 is 1.50. This low log P value indicates that compound C2 tends to be hydrophilic and has difficulty crossing lipid membranes. This is why compound C2 is unable to penetrate the BBB and CNS. Compound C2 has 6 hydrogen bond acceptors (HBA) and 4 hydrogen bond donors (HBD). Chemically, the HBA and HBD of compound C2 are facilitated by hydroxyl groups attached to rings A, B, and C of the flavonoid structure.

Table 3. Drug-likeness profile of compound C2.

Parameter	Predicted value	Unit
Log P (iLOGP)	1.50	-
Molecular weight (MW)	286.239	g/mol
HBA	6	-
HBD	4	-
Num. rotatable bonds	1	-
Topological polar surface area (TPSA)	111.13	$Å^2$
Violation of Lipinski rule	-	-
Drug-likeness score	0.46	-

The number of rotatable bonds in compound C2 is 1. This low value indicates that compound C2 is rigid. This means that the compound tends to have good oral bioavailability. Unfortunately, this rigid property slightly affects its metabolism by metabolic enzymes. This fact aligns with the metabolism prediction (Table 2). Compound C2 does not act as a substrate for either CYP2D6 or CYP3A4 enzymes. The TPSA value of compound C2 is 111.13 $Å^2$, which falls within the Lipinski rule (<140 $Å^2$). This indicates that the compound is likely to form hydrogen bonds and improve its oral bioavailability. Overall, the drug-likeness evaluation of compound C2 indicates that it does not violate the Lipinski rule. Furthermore, the drug-likeness score of compound C2 is 0.46, indicating that it exhibits good drug-like characteristics. Therefore, compound C2, in this case fisetin found in *Ageratum conyzoides* L., holds significant potential as an EGFR inhibitor, although this conclusion still needs confirmation through wet lab testing.

Conclusion

The in silico evaluation of EGFR inhibition activity has been conducted on a group of active compounds found in *Ageratum Conyzoides* L. The molecular docking results indicate that compound C2, or fisetin, exhibits the best binding energy (-8.9 kcal/mol). Fisetin's binding energy is also higher than that of erlotinib (-7.9 kcal/mol), used as a reference compound. Chemical interactions of fisetin were observed at the catalytic site of EGFR such as Met769, hydrophobic site I including Val702, and hydrophobic site II including Leu694 and Leu820. Compound C2 demonstrates good ADME properties and is non-toxic according to AMES toxicity evaluation. It also adheres to the Lipinski rule, indicating favorable drug-likeness characteristics. Therefore, compound C2 has potential as an EGFR inhibitor or anticancer agent.

Conflict of Interest

The authors declare that there is no conflict of interest.

References

Aernan, P. T., Odo, J. I., Ado, B. V., Mende, I. U., Yaji, E. M., & Iqbal, M. N. (2024). Phytochemical and Antibacterial Assessment of *Ageratum conyzoides* Cultivated in Benue State, Nigeria. *PSM Biological Research*, *9*(1), 41–50.

Banerjee, P., Kemmler, E., Dunkel, M., & Preissner, R. (2024). ProTox 3.0: A Webserver for The Prediction of Toxicity of Chemicals. *Nucleic Acids Research*, *5*(21), 1–8.

Cheng, Y.-L., Lee, C.-Y., Huang, Y.-L., *et al.* (2023). Molecular Docking in the Study of Ligand-Protein Recognition: An Overview. In *Intech.* IntechopeOpen. 1–21.

Chunaifah, I., Venilita, R. E., Tjitda, P. J. P., Astuti, E., & Wahyuningsih, T. D. (2024). Thiophene-Based N-Phenyl Pyrazolines: Synthesis, Anticancer Activity, Molecular Docking and ADME Study. *Journal of Applied Pharmaceutical Science*, *14,*(4), 63–71.

de Araújo, R. A., da Luz, F. A. C., da Costa Marinho, E., *et al*. (2022). Epidermal Growth Factor Receptor (EGFR) Expression in The Serum of Patients With Triple-Negative Breast Carcinoma: Prognostic Value of This Biomarker. *Ecancermedicalscience*, *16*(1431), 1–16.

Falcón-Cano, G., Molina, C., & Cabrera-Pérez, M. Á. (2022). Reliable Prediction of Caco-2 Permeability by Supervised Recursive Machine Learning Approaches. *Pharmaceutics*, *14*(10), 1–21.

Febriansah, R., & Komalasari, T. (2019). Co-Chemotherapeutic Effect of *Ageratum conyzoides* L. Chloroform Fraction and 5-Fluorouracil on Hela Cell Line. *Pharmacognosy Journal*, *11*(5), 913–918.

Greenblatt, D. J. (2014). Volume of Distribution-Again. *Clinical Pharmacology in Drug Development*, *3*(6), 419–420.

Hariono, M., Rollando, R., Karamoy, J., *et al*. (2020). Bioguided Fractionation of Local Plants Against Matrix Metalloproteinase9 and Its Cytotoxicity Against Breast Cancer Cell Models: In Silico and In Vitro Study. *Molecules*, *25*(20), 1–17.

Kang, K. A., Piao, M. J., Madduma Hewage, S. R. K., *et al*. (2016). Fisetin Induces Apoptosis and Endoplasmic Reticulum Stress in Human Non-Small Cell Lung Cancer Through Inhibition of The MAPK Signaling Pathway. *Tumor Biology*, *37*(7), 9615–9624.

Kementerian Kesehatan RI. (2022). *Kanker Payudara Paling Banyak di Indonesia, Kemenkes Targetkan Pemerataan Layanan Kesehatan – Sehat Negeriku*. https://sehatnegeriku.kemkes.go.id/baca/umum/20220202/1639254/kanker-payudaya-paling-banyak-di-indonesia-kemenkes-targetkan-pemerataan-layanan-kesehatan/ (accessed on 5th March 2024)

Lagares, L. M., Minovski, N., & Novič, M. (2019). Multiclass Classifier for P-Glycoprotein Substrates, Inhibitors, and Non-Active Compounds. *Molecules*, *24*(10), 1–22.

Li, Y. S., Qin, X. J., & Dai, W. (2017). Fisetin Suppresses Malignant Proliferation in Human Oral Squamous Cell Carcinoma Through Inhibition of Met/Src Signaling Pathways. *American Journal of Translational Research*, *9*(12), 5678–5683.

Mudunuru, S., Gurubilli, C. S. R., Sharma, G. V. R., & Rao, G. S. (2023). Synthesis of Biologically Active Compounds Derived from Natural Products. *International Journal of Pharmacognosy and Chemistry*, *4*(2), 1–6.

Nguyen, C. C., Nguyen, T. Q. C., Kanaori, K., *et al*. (2021). Antifungal Activities of *Ageratum conyzoides* L. Extract Against Rice Pathogens Pyricularia oryzae Cavara and Rhizoctonia solani Kühn. *Agriculture (Switzerland)*, *11*(11), 1–14.

Pires, D. E. V., Blundell, T. L., & Ascher, D. B. (2015). pkCSM: Predicting Small-Molecule Pharmacokinetic and Toxicity Properties Using Graph-Based Signatures. *Journal of Medicinal Chemistry*, *58*(9), 4066–4072.

Qi, J., Xu, G., Wu, X., Lu, C., Shen, Y., & Zhao, B. (2023). PELI1 and EGFR Cooperate to Promote Breast Cancer Metastasis. *Oncogenesis 2023 12:1*, *12*(1), 1–13.

Samuels, E. R., & Sevrioukova, I. F. (2021). Rational Design of CYP3A4 Inhibitors: A One-Atom Linker Elongation in Ritonavir-Like Compounds Leads to a Marked Improvement in the Binding Strength. *International Journal of Molecular Sciences*, *22*(2), 1–22. https://doi.org/10.3390/IJMS22020852

Sim, D. S. M. (2015). Drug Absorption and Bioavailability. In *Pharmacological Basis of Acute Care*. Springer International Publishing. 17–26

Singh, P., & Bast, F. (2014). In Silico Molecular Docking Study of Natural Compounds on Wild and Mutated Epidermal Growth Factor Receptor. *Medicinal Chemistry Research*, *23*(12), 5074–5085.

Suh, Y., Afaq, F., Johnson, J. J., & Mukhtar, H. (2009). A plant Flavonoid Fisetin Induces Apoptosis in Colon Cancer Cells by Inhibition of COX2 and Wnt/EGFR/NF-κB-Signaling Pathways. *Carcinogenesis*, *30*(2), 300–307.

Vikasari, S. N., Sukandar, E. Y., Suciati, T., & Adnyana, I. K. (2022). Antiinflammation and Antioxidant Effect of Ethanolic Extract of *Ageratum conyzoides* Leaves. in *IOP Conference Series: Earth and Environmental Science*. IOP Publishing.

WHO. (2024). *Breast cancer*. https://www.who.int/news-room/fact-sheets/detail/breast-cancer (accessed on 20th April 2024)

Yadav, N., Ganie, S. A., Singh, B., Chhillar, A. K., & Yadav, S. S. (2019). Phytochemical Constituents and Ethnopharmacological Properties of *Ageratum conyzoides* L. *Phytotherapy Research*, *33*(9), 2163–2178.

Yang, H., Zhang, Z., Liu, Q., Yu, J., Liu, C., & Lu, W. (2023). Identification of Dual-Target Inhibitors for Epidermal Growth Factor Receptor and AKT: Virtual Screening Based on Structure and Molecular Dynamics Study. *Molecules*, *28*(22), 1–21.